JYX
JYVÄSKYLÄN YLIOPISTO
UNIVERSITY OF JYVÄSKYLÄ

This is a self-archived version of an original article. This version may differ from the original in pagination and typographic details.

Author(s): Kinnunen, Virva; Frimodig, Janne; Perämäki, Siiri; Matilainen, Rose

Title: Application of 3D printed scavengers for improving the accuracy of single-particle inductively coupled plasma mass spectrometry analyses of silver nanoparticles by dissolved silver removal

Year: 2023

Version: Published version

Copyright: © 2023 The Authors. Published by Elsevier B.V.

Rights: CC BY 4.0

Rights url: https://creativecommons.org/licenses/by/4.0/

Please cite the original version:

Kinnunen, V., Frimodig, J., Perämäki, S., & Matilainen, R. (2023). Application of 3D printed scavengers for improving the accuracy of single-particle inductively coupled plasma mass spectrometry analyses of silver nanoparticles by dissolved silver removal. Spectrochimica Acta Part B: Atomic Spectroscopy, 203, Article 106662. https://doi.org/10.1016/j.sab.2023.106662

Spectrochimica Acta Part B: Atomic Spectroscopy 203 (2023) 106662

Contents lists available at ScienceDirect

Spectrochimica Acta Part B: Atomic Spectroscopy

journal homepage: www.elsevier.com/locate/sab

Application of 3D printed scavengers for improving the accuracy of single-particle inductively coupled plasma mass spectrometry analyses of silver nanoparticles by dissolved silver removal

Virva Kinnunen *, Janne Frimodig, Siiri Perämäki, Rose Matilainen

Department of Chemistry, Chemistry in Circular Economy, University of Jyväskylä, P.O. Box 35, FI-40014 Jyväskylä, Finland

ARTICLE INFO

Keywords:
SP-ICP-MS
Silver nanoparticles
Functional 3D scavengers
Dissolved silver interference
3D printing

ABSTRACT

The determination of silver nanoparticles (Ag NPs) with single-particle inductively coupled plasma mass spectrometry can be severely interfered with coexisting dissolved silver causing high background signals, which can lead to inaccurate quantification of NP size and particle concentration. In this paper, chemically active and reusable 3D printed scavengers are applied for highly efficient dissolved silver removal in Ag NP dispersions, allowing more accurate determination of particle concentration and size. Selective laser sintering was used for constructing the porous 3D scavengers constituting of polystyrene used as a supporting material and ion-exchange material SiliaBond Tosic acid (TA), which were chosen based on their high dissolved silver extraction efficiency and ability to maintain original NP properties. The macroporous structure of the final 3D TA scavengers allowed Ag NPs to pass freely through the object without affecting their original properties. The efficient contact between the sample solution and the functional material resulted in rapid (ca. <1 min/sample), and highly efficient dissolved silver removal (≥98%). The 3D TA scavengers showed potential to be used for preconcentration of dissolved silver, and the retained dissolved silver can be eluted with a 0.5 mM solution of sodium thiosulphate with excellent recoveries (≥99%). Competitive adsorption of elements commonly found in natural waters (Ca, K, Mg, Na, S, Si, and Sr) were not found to affect the dissolved silver extraction efficiency. The developed pre-treatment method was applied for the determination of 30 nm Ag NPs in ultrapure and clear environmental waters with coexisting dissolved silver (0.2 μg kg^{-1}). Whereas measurement of the samples as such led to a significant bias in NP sizing (up to +12% increase) and counting (up to −51% decrease), pre-treatment of samples with the functional 3D TA scavengers eliminated the interfering effect of dissolved silver. This resulted in significant improvement in NP detection and determination. Highly similar values were obtained for both NP mean size (30 ± 1 nm, <4% different) and concentration (<13% different) in all matrices studied as compared to samples in the absence of dissolved silver.

1. Introduction

The antimicrobial properties of silver nanoparticles (Ag NPs) are increasingly used in various applications and consumer products, which has raised concerns about their potential adverse effects on the environment and human health [1–5]. The realistic risk assessment of these materials requires sensitive analytical techniques, for which single-particle inductively coupled plasma mass spectrometry (SP-ICP-MS) has evolved as a viable alternative [6–9]. In SP-ICP-MS, the analyte intensity is recorded as a function of time using very short dwell times (e.g. ≤10 ms [6]). Whereas the ionization of the dissolved element results in a constant flow of ions to the detector and thus a relative steady-state signal, ionization of individual NPs generates a discrete pulse of ions separating from the baseline. The intensities originating from NPs can be obtained by the separation of pulse intensities over a certain threshold limit, which is typically determined using an iterative 'mean + 3σ' computation [7,10–13]. In the presence of high concentration of dissolved element, however, separation of the NP events from the background signal can prove challenging. In these cases, the dissolved signal might overlap NP pulses and lead to the computation of a threshold value being larger than some or possibly all NP signals, and thus, biased determination (overestimation of the NP size and underestimation of the

* Corresponding author.
E-mail address: virva.v-t.kinnunen@jyu.fi (V. Kinnunen).

https://doi.org/10.1016/j.sab.2023.106662
Received 13 July 2022; Received in revised form 15 March 2023; Accepted 16 March 2023
Available online 17 March 2023
0584-8547/© 2023 The Authors. Published by Elsevier B.V. This is an open access article under the CC BY license (http://creativecommons.org/licenses/by/4.0/).

particle concentration) [14,15]. The situation is particularly challenging for samples containing elevated concentrations of dissolved analyte and/or small NPs, e.g. for environmental samples [15–17].

In the presence of high concentrations of dissolved elements, the use of high data acquisition frequencies (with dwell times ≤100 μs) [7,18,19] or sophisticated mathematical models [20,21] can be used to improve the separation of NP events from the background signal. However, these methods are often found inadequate to eliminate the interfering effect of coexisting dissolved element or may require laborious manual data processing. The background signal can be decreased efficiently by physical removal of the dissolved element as well, for which several options have been suggested over the years. The simplest solution for reducing the dissolved concentration of the sample is sample dilution, as proposed by Schwertfeger et al. [16]. However, considering environmental samples with low NP concentration [2,16,17,22,23], sampling times often need to be extended to ensure the capture of a sufficient amount of NP events for reliable determination [24]. Sample dilution can also promote NP instability in highly diluted solutions [25–28], which should be avoided.

Over the years, several authors have demonstrated the beneficiation of solid phase extraction (SPE) materials for efficient separation of NPs from their ionic counterparts followed by SP-ICP-MS detection [14,15,29–31]. These materials have been used either for sample pre-treatment in off-line systems [14,30] or in-lab built columns connected directly on-line with ICP-MS [15,29,31,32]. The use of powdery SPE materials, however, can be challenging requiring either separation of the solid materials from the sample solution or time-consuming washing and regeneration steps in on-line systems (up to 60 min). These problems can be avoided by the utilization of 3D printing, which has gained great interest in a wide array of applications [33–36]. In addition to producing complex objects with precise dimensions, 3D printing technique can be used for manufacturing of objects possessing actual chemical functionalities, such as catalysts [24,37] and 3D printed scavengers used for the recovery of pharmaceuticals [38] and precious metals [39,40] from waste streams. In selective laser sintering (SLS), polymer particles used as printing material are partially sintered together to obtain an object with desired size and shape. The partial melting of the particles allows the formation of a highly porous structure with accessible voids between the sintered polymer grains, allowing the sample solution to pass through the object. The porosity, as well as other physical and mechanical properties of the 3D printed objects, can be controlled by adjusting the printing parameters (e.g. laser speed and power) [41]. An additional benefit of SLS is the wide range of materials used for printing [35], and the possibility to incorporate chemically active materials with specific desired functionalities [37,38,42,43]. Instead of using materials in their powdery form, the incorporation of SPE materials into 3D objects with fully customizable size, shape, porosity, and functionality increases their usability in a wide range of applications.

This paper presents a novel sample pre-treatment procedure using a functional 3D printed scavenger for the efficient removal of dissolved silver in NP dispersions, allowing more accurate determination of Ag NP size and concentration. The effect of 3D scavengers on Ag NP properties and their ability to extract dissolved silver is thoroughly investigated. In addition, the selectivity towards silver in the presence of various competing elements commonly found in natural waters (Ca, K, Mg, Na, S, Si, and Sr) and the adsorption behaviour of the 3D scavengers is studied. Finally, the proposed method is applied for the determination of 30 nm Ag NPs in ultrapure (UP) and clear natural waters. To the best of our knowledge, this study is the first to demonstrate the beneficiation of functional 3D scavengers for improving the accuracy of Ag NP size and concentration determination by dissolved silver removal.

2. Experimental

2.1. Materials

UP water (18.2 MΩ•cm) obtained from PURELAB Ultra water purification system (ELGA LabWater, Buckinghamshire, UK) was used for the preparation of all aqueous solutions and sample dilutions. Single-element stock solutions of silver and ruthenium (1000 mg L^{-1}) and multi-element standard solutions (29-Element and 12-Element Solution, 10 mg L^{-1}) were obtained from PerkinElmer (MA, USA). Sodium thiosulfate (STS, ≥98.0%) and thiourea (TU, ≥99.0%) were obtained from Sigma-Aldrich (Saint Louis, MO, USA). High-purity nitric (HNO_3) and hydrochloric (HCl) acids were obtained from Analytika spol. s r.o. (Prague, Chech Republic). A 1 mol L^{-1} solution of nitric acid was prepared from nitric acid (≥65%) obtained from Sigma-Aldrich. Polystyrene (PS) was obtained from Axalta Polymer Powders (Bulle, Switzerland) and SPE material SiliaBond Tosic acid (TA) from SiliCycle (Québec, Canada).

Citrate-stabilized Ag NPs with nominal sizes of 30, 40, 50, and 80 nm were obtained from NanoComposix (San Diego, CA, USA). Ultra-uniform 50 nm PEG-Carboxyl-stabilized Au NPs specially designed for SP-ICP-MS calibration were obtained from PerkinElmer. The certified values of all commercial NP dispersions were verified in the laboratory before performing any experiments. More details of the verification measurements can be found in the supplementary material (Table S1 in Appendix) and our previous publications [14,44].

Environmental water samples used in this study were collected from different locations situated in Central Finland and stored in the refrigerator at 6–8 °C until use. Before conducting any experiments, the elemental composition and other physicochemical parameters of the water samples were determined in the laboratory. More detailed information on the experimental procedure and the obtained results are presented in Tables S2 and S3 (Appendix).

2.2. Instrumentation

2.2.1. SP-ICP-MS and ICP-MS (standard mode) measurements

All ICP-MS measurements were performed using a NexION350D ICP-MS (PerkinElmer, Table S4 in Appendix) equipped with an ESI 4DX autosampler (Elemental Scientific, NE, USA). The SP-ICP-MS measurements were performed operating the instrument in single-particle mode. A commercially available Syngistix Nano Application Module software (v. 2.5) by PerkinElmer was used for SP-ICP-MS data acquisition and processing of the raw data. The software automatically discriminates the NP events from the continuous background (dissolved) signal using an intensity threshold value determined using an iterative "mean + 3σ" computation [44].

Dissolved silver calibration standards ranging from 0.1 to 2 μg kg^{-1} were prepared from a stock solution of silver (1000 mg L^{-1}). Citrate-stabilized Ag NPs with nominal sizes of 40, 50, and 80 nm were used for the preparation of the particle calibration standards. 50 nm PEG-Carboxyl-stabilized Au NPs were used for transport efficiency determination after dilution to a particle concentration of approximately 10^5 particles g^{-1} using the particle frequency method described by Pace et al. [13]. The sample flow rate was determined daily at least in duplicate by quantifying the water uptake after 3 min of aspiration. To minimize the adsorptive losses of dissolved silver onto solid surfaces [28,45,46] and eliminate any matrix interferences, the matrix of all solutions of silver (both NP and dissolved silver) were adjusted to 0.5 mM of STS before measurement.

ICP-MS operating in standard mode was used in some experiments for the concentration measurements of silver from acidified samples. Calibration standards ranging from 1 to 100 μg kg^{-1} were prepared by diluting the stock solution of silver (1000 mg L^{-1}) with a solution composed of 0.1% TU (*w/v*), 2.25% HCl (*v*/v) and 0.75% HNO_3 (v/v). ^{102}Ru was used as the internal standard. All solutions used in the

experiments were diluted gravimetrically daily prior to the experiments.

2.2.2. Scanning electron microscopy

Scanning electron microscope analysis of the 3D scavengers was conducted using Zeiss EVO-50XVP (Carl Zeiss AG, Oberkochen, Germany). Samples were plated with a thin layer of gold using a gold sputter machine to enhance conductivity and improve imaging. Images were produced using backscatter electron detection with an acceleration voltage of 20 kV and a working distance of 9.5 mm.

2.2.3. Preparation of the 3D printed scavengers

The designing of the 3D scavengers was performed using FreeCad (v. 0.16) and Slic3r (v. 1.2.9) softwares to obtain objects with desired size and shape (5 mm in height and 16.5 mm in diameter with an average mass of 0.53 g). The material used for 3D printing was prepared by manually mixing PS and TA in a mass ratio of 1:10 (10 m-% of TA), with an estimated cost of 0.25 €/3D TA scavenger (ca. 0.27 USD). The materials used for constructing the 3D TA scavengers were chosen based on their negligible effects on original NP properties (Table S5 and Fig. S1 in Appendix) and highly efficient dissolved silver extraction efficiency in clear waters [14]. The printing of the 3D scavengers was performed with a Sharebot SnowWhite SLS 3D printer (Nibionno LC, Italy) using the operational parameters shown in Table S6 (Appendix). The 3D TA scavengers were then tightly fit into 10 ml syringes (one 3D scavenger/syringe) and washed with UP water and 1 M HNO_3 to remove any unsintered material or residual impurities. Finally, all 3D scavengers were thoroughly rinsed with UP water until a neutral pH was achieved.

2.2.4. Effect of 3D TA scavengers on analyte properties and regeneration of the scavengers

The ability of the 3D TA scavengers to extract dissolved silver and their possible effect on Ag NPs properties was investigated. Dispersions containing either 1 μg kg^{-1} of dissolved silver or 10^5 part. g^{-1} of 50 nm Ag NPs were passed through a 10 ml syringe containing one 3D TA scavenger within approximately 1 min (flow rate ca. 10 ml min^{-1}). The solution containing Ag NPs was collected from the tip of the syringe into a 15 ml PP tube, whereas dissolved silver is retained in the 3D scavenger during the process. All experiments were performed in triplicate ($n = 3$). The concentration of silver (both dissolved and NP silver) was then analysed with SP-ICP-MS as described in paragraph 2.2. The effect of the 3D scavengers on Ag NP properties was evaluated by comparing the mean particle size and size distribution histograms obtained for samples before (i) and after (f) passing through the 3D scavengers and using eq. 1, where C_p is the obtained particle concentration (part. g^{-1}):

$$C_p recovery\ (\%) = \frac{C_{p(f)}}{C_{p(i)}} \bullet 100\% \quad (1)$$

The dissolved silver extraction efficiency (EE-%) of the 3D TA scavengers was calculated according to Eqs. (2) or (3), where C_{Ag} is the concentration of dissolved silver (μg kg^{-1}) before (i) and after (f) passing through the 3D TA scavenger. Limit of quantification (LOQ) of 0.02 μg kg^{-1} for silver was determined as the mean + 10*standard deviation of blank samples ($n = 50$) and considered in the calculations as follows:

$C_{Ag\ (f)} > LOQ$:

$$EE - \% = \frac{C_{Ag\ (i)} - C_{Ag\ (f)}}{C_{Ag\ (i)}} \bullet 100\% \quad (2)$$

$C_{Ag\ (f)} < LOQ$:

$$EE - \% \geq \frac{C_{Ag\ (i)} - LOQ}{C_{Ag\ (i)}} \bullet 100\% \quad (3)$$

After use, all 3D scavengers were post-treated allowing the reusability of the scavengers and to investigate the possibility to retain the adsorbed silver. First, 3D scavengers were rinsed with UP water (10 ml) to remove any sample residues, after which blank samples constituting of 10 ml of UP water were passed through the 3D scavengers within one minute to evaluate possible carry-over. Following this, the adsorbed dissolved silver was eluted using 10 ml of 0.5 mM STS solution with a flow rate of ca. 10 ml min^{-1}. The silver content of the solutions was then measured with SP-ICP-MS as described in paragraph 2.2. The desorption efficiency (DE-%) was calculated according to Eqs. 4 or 5, where $C_{Ag\ (e)}$ is the concentration of dissolved silver (μg kg^{-1}) in the elution solution and V_e and V_i are the amounts of the elution and sample solutions (in kg), respectively:

$C_{Ag\ (f)} > LOQ$:

$$DE - \% = \frac{C_{Ag\ (e)} \bullet V_e}{\left(C_{Ag\ (i)} - C_{Ag\ (f)}\right) \bullet V_i} \bullet 100\% \quad (4)$$

$C_{Ag\ (f)} < LOQ$:

$$DE - \% \geq \frac{C_{Ag\ (e)} \bullet V_e}{\left(C_{Ag\ (i)} - 0\right) \bullet V_i} \bullet 100\% \quad (5)$$

After desorption, any STS residues were rinsed off with ca. 40 ml of UP water, and the 3D TA scavengers regenerated by passing 10 ml of 1 M HNO_3 through the 3D scavengers within approximately one minute. Finally, 3D scavengers were thoroughly rinsed with UP water until a neutral pH was achieved (ca. 40 ml).

2.2.5. Selectivity experiments

The selectivity of the 3D TA scavenger towards silver in the presence of competing elements commonly found in natural waters (Ca, K, Mg, Na, S, Si, and Sr) was investigated by comparing the elemental composition of spring water (1) spiked with 1 μg kg^{-1} of dissolved silver before and after passing through the 3D TA scavenger. Experiments were performed in duplicate ($n = 2$) as described in paragraph 2.4. After extracting the sample for SP-ICP-MS, a second aliquot of the residual sample was further extracted for ICP-OES to determine the concentration of the other elements. Finally, 3D TA scavengers were treated as described in paragraph 2.4 to elute the adsorbed dissolved silver and regenerate the scavengers.

2.2.6. Breakthrough experiments

The adsorption performance of the 3D TA scavengers was studied by performing flow-through experiments. A solution containing 1 mg L^{-1} of dissolved silver was prepared in UP water and 10 ml of the solution was set aside for direct analysis to determine the initial concentration (C_0) of silver. Following this, the solution was passed through a 10 ml syringe containing one 3D TA scavenger in 6 or 10 ml portions using a peristaltic pump (Shenchen LabV1, Baoding Shenchen Precision Pump Co., Ltd., China) with a flow rate of 2 ml min^{-1}. The concentration of silver was then determined with ICP-MS (standard mode) after an appropriate dilution. Experiments were performed on duplicate samples ($n = 2$). The adsorption performance of the 3D TA scavenger was estimated by comparing the concentration of the samples passed through the 3D TA scavenger (C_e) to the initial concentration (C_0).

2.2.7. Reusability of the 3D TA scavenger

The reusability of the 3D TA scavengers was estimated by monitoring the dissolved silver extraction efficiency and the particle concentration recoveries of the 3D TA scavengers over extended time periods. As the 3D TA scavengers can be used either for dissolved silver removal in NP dispersions or potentially also for preconcentration of dissolved silver, the reusability of the scavengers was evaluated on two different occasions. Firstly, the reusability of the scavengers was estimated for the purpose of dissolved silver removal only ("short-term reusability"). Secondly, the adsorbed silver was desorbed between samples, and the 3D scavengers were exposed to the full adsorption-elution cycle ("long-term reusability").

For the evaluation of the short-term reusability, a total of 100 ml of a dispersion containing 1 μg kg^{-1} of dissolved silver and ca. 10^5 particles

g^{-1} of 50 nm Ag NPs was passed through a 10 ml syringe containing one 3D TA scavenger in 10 ml increments. Between samples, the 3D TA scavenger was rinsed with 10 ml of UP water to remove any sample residues. Following this, blank samples were taken by passing 10 ml of UP water through the syringe to monitor possible carry-over. The silver content of the samples (both NP and dissolved silver) was then measured with SP-ICP-MS. The evaluation of the long-term reusability was performed similarly as above, however, between samples the adsorbed silver was eluted using 10 ml of 0.5 mM STS solution, and the scavenger was regenerated as described in paragraph 2.4.

2.2.8. Analysis of environmental water samples

The applicability of the proposed pre-treatment method for dissolved silver removal in NP dispersions was demonstrated by analysing water samples (UP and two spring waters) spiked with 30 nm Ag NPs (10^5 part. g^{-1}) and 0 or 0.2 μg kg^{-1} of dissolved silver. To evaluate the performance of the 3D TA scavengers, samples were analysed as such and after passing through the 3D TA scavengers as described in paragraph 2.4 in triplicate ($n = 3$). For comparative purposes, samples spiked with 0.2 μg kg^{-1} of dissolved silver were analysed also from 4-fold diluted samples. In these cases, sampling times were increased to 120 s to ensure the capture of a sufficient number of NP pulses for reliable NP determination (>100 events). The silver content of all samples was then measured with SP-ICP-MS as described in paragraph 2.2.

3. Results and discussion

3.1. Effect of 3D TA scavengers on sample properties

Fig. 1 presents the effect of the 3D TA scavengers on the mean size, particle concentration, and size distribution histograms of the 50 nm Ag NPs. The highly porous structure of the 3D TA scavengers (Fig. S2 in Appendix) allows Ag NPs to pass through the object without significantly interacting with the 3D scavenger, as confirmed by the highly similar values obtained for the samples before and after passing through the 3D TA scavengers (Fig. 1). No significant changes were either observed in the size distribution histograms, confirming the suitability of the 3D TA scavengers on NP dispersions.

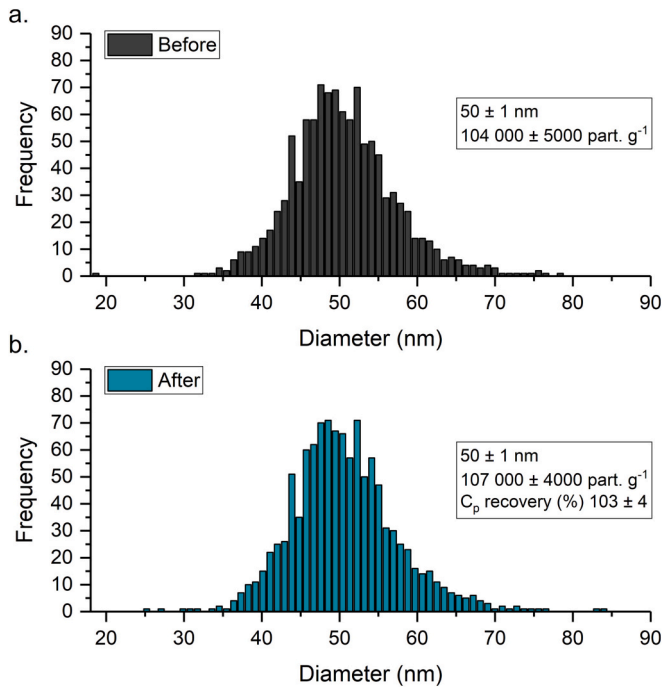

Fig. 1. The obtained values for the 50 nm Ag NP mean size and particle concentration and the size distribution histograms before (a) and after (b) passing through the 3D TA scavengers. Results are presented as a mean ± standard deviation (1 s) of three replicates ($n = 3$).

Once the 3D TA scavengers' ability to maintain the original Ag NP properties of the samples was confirmed, their dissolved silver extraction efficiency was further investigated. The macroporous structure of the 3D scavengers allowed an effective contact between the sample and the functional material, resulting in rapid (ca. 1 min/sample) and highly efficient extraction of dissolved silver (≥98%, n = 3). The dissolved silver concentrations in the solutions after passage through the 3D scavengers were near or below the LOQ of 0.02 μg kg^{-1}, indicating nearly complete adsorption. In addition, no silver was detected in the blank samples passed through the 3D TA scavengers after samples, proving that the dissolved silver was efficiently retained in the scavengers.

After confirming the suitability of the 3D TA scavengers on dissolved silver removal in NP dispersions, the possibility to desorb the adsorbed dissolved silver by elution was further investigated. STS was chosen as the most promising eluent, as it is a well-known efficient complexing agent for Ag^+ [47–49] and directly compatible with the calibration standards' matrix used in this study. Based on the preliminary studies conducted, 0.5 mM STS with 10 ml of volume was chosen as the eluent for its high efficiency and direct combability with the calibration standards (Table S7 in Appendix). Using the 0.5 mM STS solution with 10 ml of volume, excellent desorption efficiencies (≥99%, $n = 3$) were achieved. These observations indicate, that preconcentration of dissolved silver in 3D TA scavengers is possible, and efficient elution can be achieved with a 0.5 mM solution of STS.

3.2. Selectivity experiments

The selectivity of the 3D TA scavenger towards Ag was studied by investigating the competitive adsorption of various elements from a spiked spring water sample. The elemental composition of the sample before and after passing through the 3D TA scavenger is presented in Table S8 (Appendix). 3D TA scavenger was shown to extract various elements except for S and Si. Similar findings were obtained also for TA in our previous study [14], indicating that the printing process does not alter the functionality of the SPE material. The competitive adsorption of other elements was, however, not found to affect the extraction or elution efficiencies of dissolved silver, as highly efficient dissolved silver extraction (95%) and desorption efficiencies (101%) were still achieved ($n = 2$, Table S8 in Appendix). This proves the usability of the proposed method for dissolved silver removal in NP dispersion from environmental waters.

3.3. Breakthrough experiments

The experimental breakthrough curve obtained for the 3D TA scavengers using a flow rate of 2 ml min^{-1} is presented in Fig. S3 (Appendix). A gradual upward trending curve is obtained, indicating the slow saturation of the SPE materials' active sites with the increasing amount of retained silver. The 3D TA scavenger extracts dissolved silver efficiently (EE-% > 90%, i.e. $C_e/C_0 < 0.1$) until reaching the breakthrough point, which is observed after adsorption of ca. 0.10 mg of silver. After this point, the dissolved silver extraction efficiency is observed to fall below 90% (i.e., $C_e/C_0 > 0.1$), indicating the need for regeneration of the 3D TA scavenger. Eventually, full saturation is reached after the adsorption of approximately 0.60 mg of silver, after which the extraction efficiency of dissolved silver remains relatively constant (EE-% < 10%, i.e., $C_e/C_0 > 0.9$). For a 1 μg L^{-1} solution of dissolved silver, the breakthrough point would be achieved after the passage of 100 l of solution.

In samples containing other elements commonly found in natural waters (e.g. Ca and Na), the competitive binding of other elements needs to be taken into account, as these affect the capacity of the 3D TA scavenger. However, a major benefit of using 3D scavengers is that the

adsorption capacity can be easily increased by adjusting the portion of the chemically active component in the scavengers. Additionally, multiple scavengers can be used in the syringe, or the dimensions of the scavengers can be increased.

3.4. Reusability of the 3D TA scavenger

The reusability of the 3D scavengers was estimated by assessing the performance of the 3D TA scavengers over extended time periods. As seen in Fig. S4 (Appendix), 3D TA scavengers can be reused at least 10 times without a loss of dissolved silver extraction efficiency (≥98%) or significant changes in the properties of the Ag NPs. No dissolved silver nor significant amounts of particles (<5 peaks) were detected in the blank samples taken between samples, confirming the lack of significant interactions of the Ag NPs with the 3D TA scavengers, as already noticed in paragraph 3.1. Considering the long-term reusability, the 3D TA scavengers can be reused at least 5 times without affecting the functioning of the scavengers. Excellent dissolved silver extraction (≥98%) and elution (≥87%) efficiencies were achieved during the experiment, with no significant changes in NP size or concentration (Fig. S5 in Appendix).

3.5. Analysis of environmental water samples

As shown before [14,15,50], even low concentrations of dissolved silver can severely interfere with the detection of Ag NPs, leading to the inaccurate determination of these materials. As the intensity of observed NP events is related to particle mass, coexisting dissolved silver interferes foremost with the detection of the smallest NPs by increasing the size critical values [14,15,19,50,51]. Results obtained in this study confirm these observations. The presence of even 0.2 μg kg^{-1} of dissolved silver increased the size critical values from 15 nm to 19–21 nm (Table S9 in Appendix) and clearly interfered with the determination of the 30 nm Ag NPs (Fig. S6 in Appendix). As a result, a significant decrease in particle concentration (up to −51%) and an increase in particle diameter (up to +12%) was observed. The interfering effect of coexisting dissolved silver on the determination of the 30 nm Ag NPs can also be clearly seen in the size distribution histograms (Figs. S7 – S9 in Appendix). By pre-treating the samples with 3D TA scavengers, however, the interfering effect of dissolved silver can be eliminated by efficient removal of dissolved silver (≥89%, dissolved silver concentrations < LOQ, Table S10 in Appendix). This significantly improves the detection of NP events, thus allowing more accurate NP determination. When compared to samples with no added dissolved silver, highly similar values were obtained for both NP mean size (30 ± 1 nm, <4%

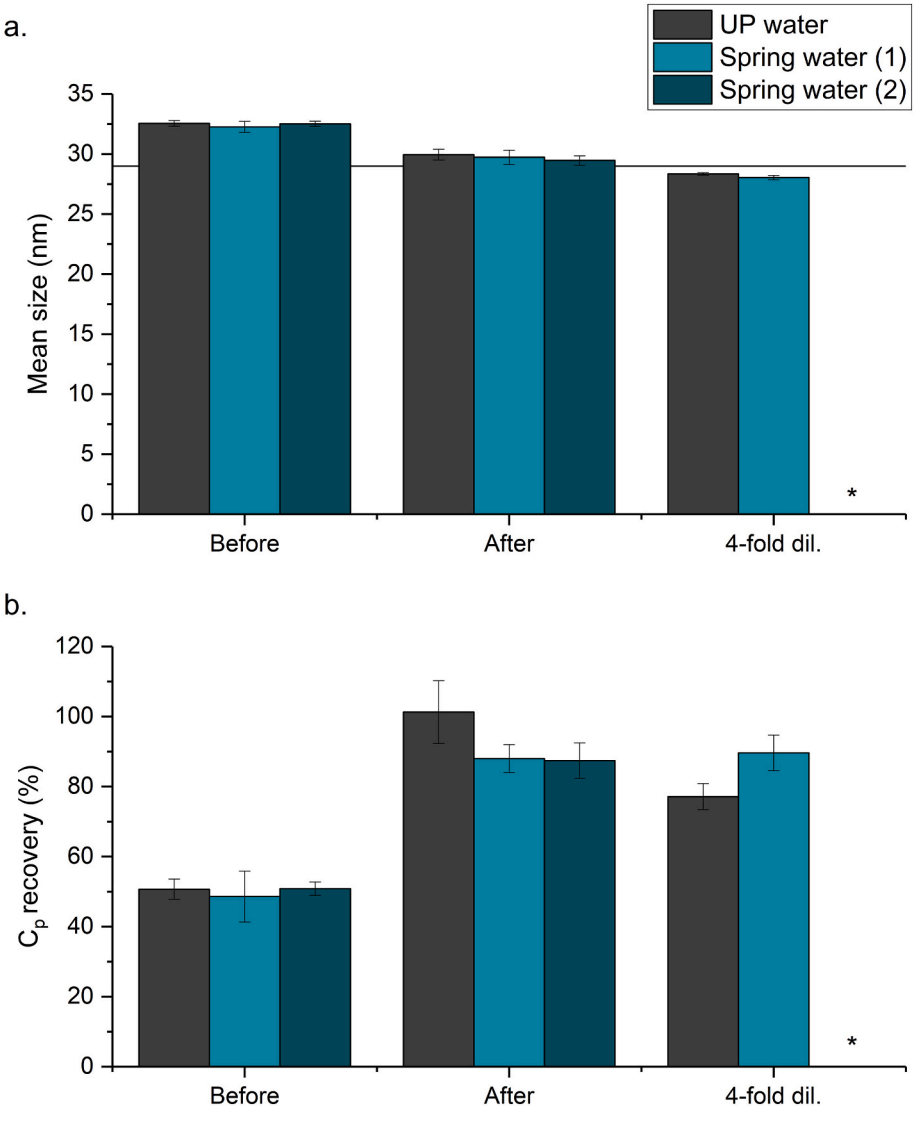

Fig. 2. The obtained results for particle mean size (a) and concentration (b) for the 30 nm Ag NP dispersions spiked with 0.2 μg kg^{-1} of dissolved silver before and after passing through the 3D TA scavenger. For comparative purposes, results are presented also for the 4-fold diluted samples. Results are given as mean ± standard deviation (1 s) of three replicates (n = 3). The reference line in Fig. 2a indicates the certified value of the 30 nm Ag NPs used in the experiments (29 ± 3 nm). Please note that the results obtained for 4-fold diluted spring water (2) sample are not shown for the occurrence of false positives (please see paragraph 10.2 in Appendix for a more detailed discussion).

different) and concentration (<13% different, Fig. 2) in all matrices studied. In addition, the adsorbed dissolved silver was recovered with satisfactory results (≥75%, Table S10 in Appendix), indicating the possibility of beneficiation of the 3D TA scavengers for preconcentration of dissolved silver in NP dispersions.

Generally, similar results were obtained for the 4-fold diluted UP and spring water (1) samples (Fig. 2), further confirming the suitability of the proposed method for dissolved silver removal in NP dispersions. However, changes in the size distribution histogram were observed for the 4-fold diluted spring water (2) sample, leading to significantly biased Ag NP determination (Fig. S9 and Table S9 in Appendix). As the observed low intensity events result presumably from the occurrence of false positives (please see paragraph 10.2 in Appendix for a more detailed discussion), these results were discarded. On the other hand, the pre-treatment of samples with the 3D TA scavengers eliminated the interfering effect of coexisting dissolved silver in all matrices while preserving the original NP properties (Figs. S7 – S9), highlighting the benefits of the proposed sample pre-treatment method. In addition, whereas the characterization of NPs in diluted samples often requires the extension of sampling times to ensure the capture of a sufficient amount of NP events [16,24,25], sample pre-treatment with the 3D TA scavengers can be performed extremely fast (ca. 1 min/sample).

4. Conclusions

This paper presents a novel sample pre-treatment method using functional 3D printed scavengers for more accurate NP determination by efficient removal of dissolved silver in Ag NP dispersions. The sample pre-treatment method proposed here offers a simple, extremely fast, and cost-effective alternative for the previously reported methods for dissolved analyte removal. The 3D printed scavengers are easy to handle, reusable, and fully customizable, allowing their widespread beneficiation in numerous applications. The 3D scavengers composed of polystyrene used as a supporting matrix and ion-exchange material SiliaBond Tosic acid (TA) were able to extract dissolved silver highly efficiently (≥98%) while maintaining the original Ag NP properties (size and concentration). The presence of various elements commonly found in natural waters (Ca, K, Mg, Na, S, Si, and Sr) was not shown to affect the 3D TA scavengers' dissolved silver extraction efficiency. In addition, the 3D TA scavengers can potentially be used for the preconcentration of dissolved silver, and efficient desorption (≥99%) can be achieved with 0.5 mM sodium thiosulfate solution. The applicability of the proposed sample pre-treatment method was further demonstrated in clear waters (ultrapure and two spring waters) containing 30 nm Ag NPs and 0.2 μg kg^{-1} of dissolved silver. Whereas measurement of samples as such resulted in significant bias in NP determination (up to +12% increase in NP sizing and up to −51% decrease in particle concentration), pre-treatment of samples with 3D TA scavengers eliminated the interfering effect of dissolved silver. This allowed more accurate determination of Ag NP concentration (<13% different) and NP mean size (30 ± 1 nm, <4% different) in all matrices studied as compared to samples in the absence of dissolved silver.

CRediT authorship contribution statement

Virva Kinnunen: Conceptualization, Validation, Formal analysis, Investigation, Visualization, Writing – original draft, Writing – review & editing. **Janne Frimodig:** Writing – original draft, Investigation, Resources. **Siiri Perämäki:** Supervision, Writing – original draft. **Rose Matilainen:** Project administration, Supervision, Writing – original draft, Writing – review & editing.

Declaration of Competing Interest

The authors declare that they have no known competing financial interests or personal relationships that could have appeared to influence the work reported in this paper.

Data availability

Data will be made available on request.

Acknowledgements

This work was supported by the University of Jyväskylä, Department of Chemistry. The authors would like to thank Joona Rajahalme and Joni Niskanen for the inspirational discussions regarding the subject and comments on the manuscript. Kaisa Lampinen and Elina Hautakangas are greatly appreciated for their help with sample preparation and Hannu Salo for SEM imaging.

Appendix A. Supplementary data

Supplementary data to this article can be found online at https://doi.org/10.1016/j.sab.2023.106662.

References

[1] E.A.J. Bleeker, S. Evertz, R.E. Geertsma, W.J.G.M. Peijnenburg, J. Westra, S.W. P. Wijnhoven, Assessing Health & Environmental Risks of Nanoparticles, National Institute for Public Health and the Environment, Bilthoven, The Netherlands, 2015.
[2] J.R. Lead, G.E. Batley, P.J.J. Alvarez, M.N. Croteau, R.D. Handy, M.J. McLaughlin, J.D. Judy, K. Schirmer, Nanomaterials in the environment: behavior, fate, bioavailability, and effects—an updated review, Environ. Toxicol. Chem. 37 (2018) 2029–2063, https://doi.org/10.1002/etc.4147.
[3] Z. Ferdous, A. Nemmar, Health impact of silver nanoparticles: a review of the biodistribution and toxicity following various routes of exposure, Int. J. Mol. Sci. 21 (2020), https://doi.org/10.3390/ijms21072375.
[4] S.P. Deshmukh, S.M. Patil, S.B. Mullani, S.D. Delekar, Silver nanoparticles as an effective disinfectant: a review, Mater. Sci. Eng. C 97 (2019) 954–965, https://doi.org/10.1016/j.msec.2018.12.102.
[5] X.F. Zhang, Z.G. Liu, W. Shen, S. Gurunathan, Silver nanoparticles: synthesis, characterization, properties, applications, and therapeutic approaches, Int. J. Mol. Sci. 17 (2016), https://doi.org/10.3390/ijms17091534.
[6] D. Mozhayeva, C. Engelhard, A critical review of single particle inductively coupled plasma mass spectrometry – a step towards an ideal method for nanomaterial characterization, J. Anal. At. Spectrom. 35 (2020) 1740–1783, https://doi.org/10.1039/c9ja00206e.
[7] B. Meermann, V. Nischwitz, ICP-MS for the analysis at the nanoscale - a tutorial review, J. Anal. At. Spectrom. 33 (2018) 1432–1468, https://doi.org/10.1039/C8JA00037A.
[8] E. Bolea, M.S. Jimenez, J. Perez-Arantegui, J.C. Vidal, M. Bakir, K. Ben-Jeddou, A. C. Gimenez-Ingalaturre, D. Ojeda, C. Trujillo, F. Laborda, Analytical applications of single particle inductively coupled plasma mass spectrometry: a comprehensive and critical review, Anal. Methods 13 (2021) 2742–2795, https://doi.org/10.1039/d1ay00761k.
[9] F. Laborda, E. Bolea, G. Cepriá, M.T. Gómez, M.S. Jiménez, J. Pérez-Arantegui, J. R. Castillo, Detection, characterization and quantification of inorganic engineered nanomaterials: a review of techniques and methodological approaches for the analysis of complex samples, Anal. Chim. Acta 904 (2016) 10–32, https://doi.org/10.1016/j.aca.2015.11.008.
[10] M.D. Montaño, J.W. Olesik, A.G. Barber, K. Challis, J.F. Ranville, Single particle ICP-MS: advances toward routine analysis of nanomaterials, Anal. Bioanal. Chem. 408 (2016) 5053–5074, https://doi.org/10.1007/s00216-016-9676-8.
[11] C. Degueldre, P.Y. Favarger, Colloid analysis by single particle inductively coupled plasma-mass spectroscopy: a feasibility study, Colloids Surf. A Physicochem. Eng. Asp. 217 (2003) 137–142, https://doi.org/10.1016/S0927-7757(02)00568-X.
[12] F. Laborda, J. Jiménez-Lamana, E. Bolea, J.R. Castillo, Selective identification, characterization and determination of dissolved silver(i) and silver nanoparticles based on single particle detection by inductively coupled plasma mass spectrometry, J. Anal. At. Spectrom. 26 (2011) 1362–1371, https://doi.org/10.1039/c0ja00098a.
[13] H.E. Pace, N.J. Rogers, C. Jarolimek, V.A. Coleman, C.P. Higgins, J.F. Ranville, Determining transport efficiency for the purpose of counting and sizing nanoparticles via single particle inductively coupled plasma mass spectrometry, Anal. Chem. 83 (2011) 9361–9369, https://doi.org/10.1021/ac201952t.
[14] V. Kinnunen, S. Perämäki, R. Matilainen, Solid phase extraction materials as a key for improving the accuracy of silver nanoparticle characterization with single-particle inductively coupled plasma mass spectrometry in natural waters through dissolved silver removal, Spectrochim Acta Part B At Spectrosc. 193 (2022), 106431, https://doi.org/10.1016/j.sab.2022.106431.
[15] M. Hadioui, C. Peyrot, K.J. Wilkinson, Improvements to single particle ICPMS by the online coupling of ion exchange resins, Anal. Chem. 86 (2014) 4668–4674, https://doi.org/10.1021/ac5004932.

[16] D.M. Schwertfeger, J.R. Velicogna, A.H. Jesmer, R.P. Scroggins, J.I. Princz, Single particle-inductively coupled plasma mass spectroscopy analysis of metallic nanoparticles in environmental samples with large dissolved Analyte fractions, Anal. Chem. 88 (2016) 9908–9914, https://doi.org/10.1021/acs.analchem.6b02716.
[17] K. Newman, C. Metcalfe, J. Martin, H. Hintelmann, P. Shaw, A. Donard, Improved single particle ICP-MS characterization of silver nanoparticles at environmentally relevant concentrations, J. Anal. At. Spectrom. 31 (2016) 2069–2077, https://doi.org/10.1039/c6ja00221h.
[18] F. Laborda, J. Jiménez-Lamana, E. Bolea, J.R. Castillo, Critical considerations for the determination of nanoparticle number concentrations, size and number size distributions by single particle ICP-MS, J. Anal. At. Spectrom. 28 (2013) 1220–1232, https://doi.org/10.1039/c3ja50100k.
[19] F. Laborda, A.C. Gimenez-Ingalaturre, E. Bolea, J.R. Castillo, About detectability and limits of detection in single particle inductively coupled plasma mass spectrometry, Spectrochim Acta Part B At Spectrosc. 169 (2020), 105883, https://doi.org/10.1016/j.sab.2020.105883.
[20] D. Mozhayeva, C. Engelhard, A quantitative nanoparticle extraction method for microsecond time resolved single-particle ICP-MS data in the presence of a high background, J. Anal. At. Spectrom. 34 (2019) 1571–1580, https://doi.org/10.1039/c9ja00042a.
[21] A. Gundlach-Graham, L. Hendriks, K. Mehrabi, D. Günther, Monte Carlo simulation of low-count signals in time-of-flight mass spectrometry and its application to single-particle detection, Anal. Chem. 90 (2018) 11847–11855, https://doi.org/10.1021/acs.analchem.8b01551.
[22] B. Giese, F. Klaessig, B. Park, R. Kaegi, M. Steinfeldt, H. Wigger, A. von Gleich, F. Gottschalk, Risks, release and concentrations of engineered nanomaterial in the environment, Sci Rep. 8 (2018) 1–18, https://doi.org/10.1038/s41598-018-19275-4.
[23] T.Y. Sun, N.A. Bornhöft, K. Hungerbühler, B. Nowack, Dynamic probabilistic modeling of environmental emissions of engineered nanomaterials, Environ. Sci. Technol. 50 (2016) 4701–4711, https://doi.org/10.1021/acs.est.5b05828.
[24] E. Lahtinen, E. Kukkonen, V. Kinnunen, M. Lahtinen, K. Kinnunen, S. Suvanto, A. Vaïsänen, M. Haukka, Gold nanoparticles on 3D-printed filters: from waste to catalysts, ACS Omega. 4 (2019) 16891–16898, https://doi.org/10.1021/acsomega.9b02113.
[25] K.E. Murphy, J. Liu, A.R. Montoro, B.M.E. Johnson, M.R. Winchester, Characterization of nanoparticle suspensions using single particle inductively coupled plasma mass spectrometry, in: NIST Special Publication 1200-21, 2011, pp. 1200–1221, https://doi.org/10.6028/NIST.SP.1200-21.
[26] I. Römer, T.A. White, M. Baalousha, K. Chipman, M.R. Viant, J.R. Lead, Aggregation and dispersion of silver nanoparticles in exposure media for aquatic toxicity tests, J. Chromatogr. A 1218 (2011) 4226–4233, https://doi.org/10.1016/j.chroma.2011.03.034.
[27] J. Wan, Y. Kim, M.J. Mulvihill, T.K. Tokunaga, Dilution destabilizes engineered ligand-coated nanoparticles in aqueous suspensions, Environ. Toxicol. Chem. 37 (2018) 1301–1308, https://doi.org/10.1002/etc.4103.
[28] J. Liu, K.E. Murphy, M.R. Winchester, V.A. Hackley, Overcoming challenges in single particle inductively coupled plasma mass spectrometry measurement of silver nanoparticles, Anal. Bioanal. Chem. 409 (2017) 6027–6039, https://doi.org/10.1007/s00216-017-0530-4.
[29] P. Cervantes-Avilés, Y. Huang, A.A. Keller, Multi-technique approach to study the stability of silver nanoparticles at predicted environmental concentrations in wastewater, Water Res. 166 (2019), https://doi.org/10.1016/j.watres.2019.115072.
[30] L. Fréchette-Viens, M. Hadioui, K.J. Wilkinson, Quantification of ZnO nanoparticles and other Zn containing colloids in natural waters using a high sensitivity single particle ICP-MS, Talanta. 200 (2019) 156–162, https://doi.org/10.1016/j.talanta.2019.03.041.
[31] M. Hadioui, V. Merdzan, K.J. Wilkinson, Detection and characterization of ZnO nanoparticles in surface and waste waters using single particle ICPMS, Environ. Sci. Technol. 49 (2015) 6141–6148, https://doi.org/10.1021/acs.est.5b00681.
[32] L. Fréchette-Viens, M. Hadioui, K.J. Wilkinson, Practical limitations of single particle ICP-MS in the determination of nanoparticle size distributions and dissolution: case of rare earth oxides, Talanta. 163 (2017) 121–126, https://doi.org/10.1016/j.talanta.2016.10.093.
[33] H. Agrawaal, J.E. Thompson, Additive manufacturing (3D printing) for analytical chemistry, Talanta Open. 3 (2021), 100036, https://doi.org/10.1016/j.talo.2021.100036.
[34] B. Gross, S.Y. Lockwood, D.M. Spence, Recent advances in analytical chemistry by 3D printing, Anal. Chem. 89 (2017) 57–70, https://doi.org/10.1021/acs.analchem.6b04344.
[35] B.C. Gross, J.L. Erkal, S.Y. Lockwood, C. Chen, D.M. Spence, Evaluation of 3D printing and its potential impact on biotechnology and the chemical sciences, Anal. Chem. 86 (2014) 3240–3253, https://doi.org/10.1021/ac403397r.
[36] U. Kalsoom, P.N. Nesterenko, B. Paull, Current and future impact of 3D printing on the separation sciences, TrAC Trends Anal. Chem. 105 (2018) 492–502, https://doi.org/10.1016/j.trac.2018.06.006.
[37] E. Lahtinen, L. Turunen, M.M. Hänninen, K. Kolari, H.M. Tuononen, M. Haukka, Fabrication of porous hydrogenation catalysts by a selective laser sintering 3D printing technique, ACS Omega. 4 (2019) 12012–12017, https://doi.org/10.1021/acsomega.9b00711.
[38] J. Frimodig, A. Autio, E. Lahtinen, M. Haukka, Recovery of 17β-Estradiol using 3D printed polyamide-12 scavengers, 3D Print Addit Manuf. (2022), https://doi.org/10.1089/3dp.2021.0063.
[39] E. Lahtinen, M.M. Hänninen, K. Kinnunen, H.M. Tuononen, A. Väisänen, K. Rissanen, M. Haukka, Porous 3D printed scavenger filters for selective recovery of precious metals from electronic waste, Adv Sustain Syst. 2 (2018) 1–5, https://doi.org/10.1002/adsu.201800048.
[40] E. Lahtinen, L. Kivijärvi, R. Tatikonda, A. Väisänen, K. Rissanen, M. Haukka, Selective recovery of gold from electronic waste using 3D-printed scavenger, ACS Omega. 2 (2017) 7299–7304, https://doi.org/10.1021/acsomega.7b01215.
[41] S.F.S. Shirazi, S. Gharehkhani, M. Mehrali, H. Yarmand, H.S.C. Metselaar, N. Adib Kadri, N.A.A. Osman, A review on powder-based additive manufacturing for tissue engineering: selective laser sintering and inkjet 3D printing, Sci Technol, Adv. Mater. 16 (2015) 1–20, https://doi.org/10.1088/1468-6996/16/3/033502.
[42] S. Kulomäki, E. Lahtinen, S. Perämäki, A. Väisänen, Preconcentration and speciation analysis of mercury: 3D printed metal scavenger-based solid-phase extraction followed by analysis with inductively coupled plasma mass spectrometry, Talanta. 240 (2022), https://doi.org/10.1016/j.talanta.2021.123163.
[43] S. Kulomäki, E. Lahtinen, S. Perämäki, A. Väisänen, Determination of mercury at picogram level in natural waters with inductively coupled plasma mass spectrometry by using 3D printed metal scavengers, Anal. Chim. Acta 1092 (2019) 24–31, https://doi.org/10.1016/j.aca.2019.09.075.
[44] V. Kinnunen, S. Perämäki, R. Matilainen, Optimization of instrumental parameters for improving sensitivity of single particle inductively-coupled plasma mass spectrometry analysis of gold, Spectrochim Acta Part B At Spectrosc. 177 (2021), https://doi.org/10.1016/j.sab.2021.106104.
[45] R. Sekine, K. Khurana, K. Vasilev, E. Lombi, E. Donner, Quantifying the adsorption of ionic silver and functionalized nanoparticles during ecotoxicity testing: test container effects and recommendations, Nanotoxicology. 9 (2015) 1005–1012, https://doi.org/10.3109/17435390.2014.994570.
[46] W. Chen, P. Wee, I.D. Brindle, Elimination of the memory effects of gold, mercury and silver in inductively coupled plasma atomic emission spectroscopy, J. Anal. At. Spectrom. 15 (2000) 409–413, https://doi.org/10.1039/A908658G.
[47] I. López-García, Y. Vicente-Martínez, M. Hernández-Córdoba, Speciation of silver nanoparticles and Ag(I) species using cloud point extraction followed by electrothermal atomic absorption spectrometry, Spectrochim Acta Part B At Spectrosc. 101 (2014) 93–97, https://doi.org/10.1016/j.sab.2014.07.017.
[48] J.F. Liu, J.B. Chao, R. Liu, Z.Q. Tan, Y.G. Yin, Y. Wu, G. Bin Jiang, Cloud point extraction as an advantageous preconcentration approach for analysis of trace silver nanoparticles in environmental waters, Anal. Chem. 81 (2009) 6496–6502, https://doi.org/10.1021/ac900918e.
[49] J. Soto-Alvaredo, M. Montes-Bayón, J. Bettmer, Speciation of silver nanoparticles and silver(I) by reversed-phase liquid chromatography coupled to ICPMS, Anal. Chem. 85 (2013) 1316–1321, https://doi.org/10.1021/ac302851d.
[50] A.C. Gimenez-Ingalaturre, K. Ben-Jeddou, J. Perez-Arantegui, M.S. Jimenez, E. Bolea, F. Laborda, How to trust size distributions obtained by single particle inductively coupled plasma mass spectrometry analysis, Anal. Bioanal. Chem. (2022), https://doi.org/10.1007/s00216-022-04215-z.
[51] H.E. Pace, N.J. Rogers, C. Jarolimek, V.A. Coleman, E.P. Gray, C.P. Higgins, J. F. Ranville, Single particle inductively coupled plasma-mass spectrometry: a performance evaluation and method comparison in the determination of nanoparticle size, Environ. Sci. Technol. 46 (2012) 12272–12280, https://doi.org/10.1021/es301787d.